IPNO DRE 86.16

DAMPING OF HIGH-SPIN SINGLE-PARTICLE STRENGTHS IN ^{209}Pb

C.P. Massolo*, F. Azaiez**, S. Galès, S. Fortier, E. Gerlic, J. Guillot, E. Hourani and J.M. Maison

Institut de Physique Nucléaire, B.P. n° 1 - 91406 Orsay Cédex, France

UNIVERSITÉ PARIS-SUD
I.P.N. BP n» 1 - 91406 ORSAY

IPNO DRE 86.16

DAMPING OF HIGH-SPIN SINGLE-PARTICLE STRENGTHS IN ^{209}Pb

C.P. Massolo*, F. Azaiez**, S. Galès, S. Fortier, E. Gerlic, J. Guillot,
E. Hourani and J.M. Maison

Institut de Physique Nucléaire, B.P. n° 1 - 91406 Orsay Cédex, France

To be published in Physical Review C

DAMPING OF HIGH-SPIN SINGLE-PARTICLE STRENGTHS IN ^{209}Pb

C.P. Massolo*, F. Azaiez**, S. Galès, S. Fortier, E. Gerlic,
J. Guillot, E. Hourani and J.M. Maison

Institut de Physique Nucléaire, B.P. N°1 - 91406 Orsay Cedex FRANCE

Nuclear reactions : ^{208}Pb $(\alpha,^3He)$, E = 183 MeV ; measured $\sigma(E_x,\theta)$; DWBA analysis for bound and unbound states ; ^{209}Pb deduced E_x, ℓ, $(J)^\pi$, strength functions for high-lying states. Enriched target ; magnetic spectrometer ; resolution 200 keV.

Nuclear models : Comparison of neutron single-particle strength functions with the prediction of the core-particle and quasiparticle nuclear models.

ABSTRACT :

The stripping reaction $(\alpha,^3He)$ at 183 MeV incident energy has been used to study the neutron-particle response function on ^{208}Pb target nucleus up to 15 MeV excitation energy. Detailed spectroscopic information has been obtained on the low-lying neutron states (0-4 MeV) through angular distribution measurements and standard distorted wave Born approximation analysis.

A large enhancement of cross section is observed between 5 and 15 MeV. It appears as a broad bump superimposed on a continuous background which has been analysed within the framework of the plane wave break-up model. The excitation energies, angular distributions

and strengths of these high-lying transitions suggest that they arise from neutron stripping to high-spin outer subshells, i.e. $2h_{11/2}$, $1k_{17/2}$ and $1j_{13/2}$ in ^{209}Pb.

The results are compared with predictions from the core-particle model and from the quasiparticle-phonon model.

I - INTRODUCTION

A large amount of theoretical and experimental work has been devoted to the study of shell model single-particle (hole) states in the nuclei adjacent to doubly magic ^{208}Pb. In particular, the fragmentation of high-spin orbitals of ^{209}Pb is a matter of considerable interest. Most of the existing experimental data on neutron particle strength functions come from earlier (d,p)[1] and $(\alpha,^3He)$[2] studies, carried out at low bombarding energy, where the fragmentation of the $1j_{15/2}$ valence state has been observed. Above 4 MeV excitation energy, nearly no experimental information is available.

The one nucleon transfer reaction approach has been quite successful in probing high-lying proton[3,4] and neutron[5] strength distributions. Recently, the residual energy spectra from the $^{116,118,120}Sn(\alpha,^3He)$ reactions at 183 MeV incident energy[5] revealed pronounced and systematic structures up to fairly high excitation energies (5-10 MeV) which arise from neutron stripping to high-spin orbitals belonging to the next major shell above the Fermi sea. We report here on a similar study of high-spin neutron

states using the $(\alpha,{}^3He)$ reaction at 183 MeV incident energy on ^{208}Pb target. The strong selectivity of this reaction for high-ℓ transfer and the relatively good energy resolution are well suited to the investigation of the single-particle response function up to high excitation energies ($\sim$ 15 MeV). After a brief description of the experimental method (section II), the results and analysis are presented in section III. Along with the detailed information on valence-particle state fragmentation, our results provide evidence on single-particle strength distribution from the second neutron shell above the Fermi sea, i.e. the hjkf shell with neutron number $N > 184$. In section IV, the empirical determination of the high-spin states fragmentation will be compared to the predictions from the core-particle and the quasiparticle-phonon nuclear models.

II - EXPERIMENTAL PROCEDURE

The experiment was performed with an α-particle beam of 183 MeV delivered by the K 220 Orsay Synchrocyclotron. We used isotopically enriched ^{208}Pb target (99.9 %) of 10 mg/cm^2. With the beam transport system set in an achromatic mode, we obtained a current of 50-400 nA and an overall energy resolution of 200 keV, mainly determined by the target thickness. The emerging particles were detected by two multiwire proportional chambers placed at the focal plane of the large magnetic spectrometer Montpellier[6]. Following the position detectors, two plastic scintillators (3 and 5 mm thick) were used to provide the time-of-flight and energy loss signals necessary for a clean identification of the ^3He particles. The absolute cross-sections were determined using the known values of the target thickness and of the spectrometer solid angle. The error in the absolute

cross-section scales is estimated to be of the order of ± 10 %. An excitation energy range of 30 MeV has been explored using three successive exposures at different magnetic fields. The excitation energy of the observed levels has been determined from calibration of the detectors using the known energies of the low-lying states of ^{209}Pb and some strong states from neutron stripping reactions on ^{12}C and ^{16}O measured with a Mylar target. A complete angular distribution was measured from 2.5° to 15° laboratory angle in 2° steps.

III - EXPERIMENTAL RESULTS AND ANALYSIS

The ^{209}Pb energy spectrum from the (α,^{3}He) reaction taken at a laboratory angle of 8° is presented in fig. 1. One observes the low-lying levels with a very strong population of the $1j_{15/2}$ main fragment this demonstrating the selectivity of the (α,^{3}He) process for large ℓ-values (ℓ=9 at 10 MeV). The fragmented componets of the $1j_{15/2}$ subshell are clearly seen in the energy range 3-4 MeV (peaks labelled 5,6 and 7 in fig. 1). The nuclear levels of ^{209}Pb up to 4.2 MeV excitation energy are listed in table I where the spectroscopic strengths for the observed states, deduced from the DWBA analysis (see sect. IV), are compared to previous neutron stripping experiments[1,2] and theoretical predictions[19,22]. From 4.5 to 15 MeV excitation energy, the spectrum is dominated by a wide bump located around 10.7 MeV. As it will be shown later, this large enhancement of cross-section arises from neutron stripping to high-spin outer subshells, namely $2h_{11/2}$, $1j_{13/2}$ and $1k_{17/2}$.

The high energy part (15-30 MeV) of the spectrum does not exhibit pronounced structures. The shape and magnitude of the cross-section in this energy range is very similar to the one obtained from the study of the same reaction, i.e. (α,^{3}He) on ^{90}Zr, ^{120}Sn and ^{197}Au targets[7]. The weak dependance of the high-energy continuum versus the atomic number A of the target leads us to assume that the main part of the cross-section comes from the break-up of the α-particle. Wu et al.[8] and Budzanowski et al.[9] have shown that break-up processes give an important contribution to the reaction cross-section of fast α-particles scattered on heavy-weight nuclei. A simple Serber model[10,11] has been used to evaluate the direct break-up part of the reaction cross-section. The theoretical prediction was normalized to the experimental data at laboratory angle $\theta = 8°$ and at high excitation energy (E_x = 28 MeV) to minimize the contribution from other mechanisms. The result of this simple plane-wave break-up model (PWBU) is shown as a solid line in fig. 1 and was used in order to deduce the cross-section of the high-lying states. However, a sizable fraction of the cross-section located between 15 and 25 MeV excitation energy (see fig. 1) cannot be explained by the elastic break-up process. Our estimate of the background cross-section does not take into account the inelastic break-up processes in which a subset of the projectil (in this case the ^{3}He particle) interacts strongly with the target while the remaining fragment acts as a spectator. Therefore, no attempt was made to unravel the remaining part of the observed continuum in an inelastic break-up and a stripping components.

The distorted wave Born approximation (DWBA) calculations were carried out using the code DWUCK4[12]. The optical parameters employed for generating distorted waves in the entrance (α) channel were the fixed geometry "deep family" combination derived from the elastic scattering analysis on the ^{208}Pb target at 140 MeV incident energy[13]. The ^{3}He exit channel was described using the set of parameters from Ojaloeis et al.[14] which were found to reproduce quite well the elastic scattering results at 130 MeV on ^{90}Zr, ^{120}Sn and ^{208}Pb targets. Standard energy separation procedure and geometry (r = 1.25 fm, a = 0.65 fm) have been used to evaluate the bound-state neutron form factor. The optical potential parameters employed in the DWBA analysis are listed in table II.

The calculations were carried out in the local zero range (LZR) approximation, without non-locality corrections. The comparison between the experimental data and DWBA predictions, for the low-lying well resolved states, are shown in fig. 2. An excellent agreement is found between the shape of the DWBA curves and the experimental angular distributions for angular momentum transfers ranging from ℓ = 4 to ℓ = 8. Moreover, exact finite range (EFR) calculations were performed for the same transitions using the code MARY written by CHant and Graig[15]. We find that the LZR and EFR calculations produce nearly identical shapes. Furthermore, the ratio of cross-sections EFR/LZR is state and energy independant to within 10 % for the chosen set of optical potentials. Therefore, ZR-DWBA calculations were performed by using a ZR normalization constant N = 36 which is consistent with the result of EFR calculations and agrees with previous determinations of the volume integral

D_0 = 290 - 310 MeV $fm^{3/2}$ for the (α,t) and (α,^{3}He) reactions[16,17].

The observed gross structure around 10.7 MeV being located well above the neutron threshold (Sn = 3.94 MeV), a series of calculations were made using the resonance method[12,18] in order to evaluate the form factor of the unbound neutrons.

In the excitation energy range between 4.5 and 15 MeV the spectra were divided into adjacent slices 500 KeV width. Typical angular distributions of slices are shown in fig. 3. A very good agreement is found between the experimental results and DWBA calculations if one assumes a mixed transfer ℓ = 5 and ℓ = 7 in the excitation energy range 4.5 - 6.5 MeV. Although the observed difference between ℓ = 7 and ℓ = 8 transfers is rather small, an ℓ = 7 transfer fits the best the slices located between 6.5 and 9 MeV while from 11 to 15 MeV, the ℓ = 8 transfer better reproduces the trend of the experimental data. In between these regions (9-11 MeV), the best fits of the angular distributions are obtained assuming a mixed ℓ = 7 and ℓ = 8 transfer. We also show in fig. 3 the angular distribution of the under-lying background for typical energy region. The error bars on the extracted differential cross-sections are statistical errors plus a systematic error introduced by the choice of the normalization procedure of the background yield to the PWBU model prediction at 8°. In other words, the choice of another forward angle (4°, for example) will lead to slightly different background yield. This procedure leads to an additional systematic error of the order of 10 %.

IV - STRENGTH DISTRIBUTIONS AND COMPARISON TO NUCLEAR MODELS

A) LOW AND INTERMEDIATE EXCITATION ENERGY REGION < 0 - 4.5 MeV >

The deduced spectroscopic strengths for levels lying between the ground state and 4.2 MeV excitation energy are displayed in table I. They are in good agreement with previous determination from an $(\alpha,{}^3He)$ experiment carried out at lower incident energy (58 MeV) reported by Tickle and Gray[2], although different optical potential parameters and ZR normalization constant have been used. The relatively low spectroscopic strength observed for the $2g_{9/2}$ ground state is probably due to the mismatch of the $(\alpha,{}^3He)$ reaction for low-ℓ transfer. Another important fragment $\ell = 4$ $(2g_{7/2})$ state is found at 2.5 MeV in agreement with previous (d,p) experiments[1].

We compare our results for the first four low-lying states with theoretical predictions from the quasiparticle-phonon nucleon model (QPM) recently reported by Stoyanov et al.[19]. The calculations - in which a quasiparticle - phonon interaction based on the microscopic structure of the ^{208}Pb phonons is used are in good agreement with the experiment.

At 3.05, 3.59 and 3.73 MeV excitation energies, three fragments of the $1j_{15/2}$ single neutron state are clearly seen. The fragmentation of the $1j_{15/2}$ shell model state based on a weak-coupling model calculation, has been predicted by Homamoto[20] and Bes and Broglia[21]. Both calculations predict that more than 35 % of the total $1j_{15/2}$ strength is to be found between 3.2 and 3.5 MeV excitation energy. This is far too much than what is experimentally found. We have displayed in table I the core-particle

model prediction reported by Mukherjee et al.[22] where the coupling of particle motion with 3^-, 5^-, 2^+, 4^+ and 6^+ states of ^{208}Pb core have been considered. Our results are in reasonable agreement with this theoretical prediction.

Two levels at 3.96 and 4.22 MeV are clearly seen in our experiment. Their excitation energies and the spectroscopic strengths that we find assuming an $\ell = 8$ transfer are in very good agreement with the theoretical prediction of the core-particle model. Nevertheless, the similarity between the anqular distributions for $\ell = 7$ and $\ell = 8$ transfer does not allow a definite ℓ - assignment for these two levels.

8) THE HIGH EXCITATION ENERGY REGION < 4.5 - 15 MeV >

Hartree-Fock calculations predict the following high-spin subshells in this energy range : $2h_{11/2}$, $1j_{13/2}$, $1k_{17/2}$, $2h_{9/2}$ and $3f_{7/2}$. Due to the matching conditions, the expected cross-section for the $2h_{9/2}$ and $3f_{7/2}$ subshells are one order of magnitude smaller than the others around 10 MeV excitation energy. In the following we will only consider the $2h_{11/2}$, $1j_{13/2}$ and $1k_{17/2}$ subshells.

A mixing of $\ell = 5$ and $\ell = 7$ strengths is observed from 4.5 to 6.5 MeV excitation energy. Although in a limited amount (around 20 to 30 %), the addition of the $\ell = 5$ component clearly improves the fits in this energy region, but only 30 % of the sum rule is found for the $2h_{11/2}$ neutron orbital. It should be mentioned for complitness that a pure $\ell = 5$ transfer does not reproduce the experimental trend. Concerning the $\ell = 7$ component, since the analysis of the low-lying levels has shown that 72 % of the $1j_{15/2}$ strength is located below 4.5 MeV, the remaining part of the strength must

be spread over higher excitation energy. If one assumes that the $\ell = 7$ transfer corresponds to the $1j_{15/2}$ orbit, then the sum-rule limit is reached at 6.5 MeV. But very probably, a large overlap of both $1j_{15/2}$ and $1j_{13/2}$ strengths takes place in this energy region.

From 6.5 to 9 MeV the best fits are found assuming a pure $\ell = 7$ transfer while at higher excitation energy, up to 11 MeV, a mixing of $\ell = 7$ and $\ell = 8$ strengths is observed. The total amount of $1j_{13/2}$ strength that we find in the energy range 6.5 - 11 MeV is much larger than the sum-rule limit (1.79 instead of 1) within the experimental cross-section uncertainties (20 %).

Between 11 to 15 MeV excitation energy, a pure $\ell = 8$ transfer reproduces well the experimental trend. Our results show that the $\ell = 8$ strength is spread over a wide energy range (9 to 15 MeV) where 62 % of the strength is found. If one considers a pure $\ell = 8$ or $\ell = 7$ transfer, the total amount of strength located between 4.5 and 15 MeV largely exceeds the sum-rule limit (see (d) in table III).

Theoretical predictions for the high-spin high-lying subshells ($2h_{11/2}$, $1j_{13/2}$ and $1k_{17/2}$, using the quasiparticle-phonon nuclear model, and the strength function method have been reported recently by Vdovin and Stoyanov[19]. The results of the calculated strengths functions for the high-lying single-neutron states in ^{209}Pb are shown in table III and fig. 4a. Their calculations show that all the subshells are strongly fragmented.

Our results agree with the theoretical pattern of the quasi-bound part of the single-neutron scheme, i.e. two subshells with high ℓ-numbers located close to each other and a subshell with a

lower ℓ-number several MeV below them (see fig. 4a). The strength distributions of the high-ℓ subshells are predicted to be strongly overlaping as it is found experimentally. This conclusion is confirmed by the comparison made in fig. 4b between the experimental spectrum (background substracted) taken at 4° and the corresponding theoretical spectrum obtained by adding up the $2h_{11/2}$, $1k_{17/2}$ and $1j_{13/2}$ strength distrioutions and converting them through the DWUCK calculation into a double differential cross-section (mb/sr MeV). The experimental distribution is in good agreement with this build-up theoretical spectrum and demonstrates the strong overlap between the $2h_{11/2}$, $1j_{13/2}$ and $1k_{17/2}$ neutron strength functions in that energy range. The damping of these high-lying orbitals seem to be much larger than the ones predicted theoretically although the overlapping regions and the similarity between $\ell = 7$ and $\ell = 8$ angular distributions does not allow the extraction of individual strength distributions from the experimental data.

V - SUMMARY AND CONCLUSIONS

The investigation of a large excitation energy range with adequate energy resolution and good statistics has allowed a rather complete description of both low and high-lying neutron states in ^{209}Pb.

The $(\alpha,{}^3He)$ reaction appears to be a good tool for nuclear studies of high-spin orbitals. Our results confirm the core-particle predictions for the fragmentation of the $1j_{15/2}$ neutron state and two low-lying components of the $1k_{17/2}$ strength are observed between 3 and 4 MeV.

The large enhancement of cross-section observed from 5 to 15 MeV excitation energy arises from neutron stripping to the second shell above the Fermi sea, namely to the $2h_{11/2}$, $1j_{13/2}$ and $1k_{17/2}$ orbitals. The $1k_{17/2}$ neutron subshell is the single-particle orbital with the highest spin ever observed in a one nucleon transfer reaction. The strength distribution of the high-ℓ subshells are strongly overlapped. The high-lying states are spread over a large energy range and are highly damped indicating a high density of adjacent complicated states and a strong coupling with the grass states.

In the near future, exclusive experiments which look for example for the neutron decay of the high-lying states will certainly lead to decisive progress on the understanding of the very large spreading observed experimentally as compared to tne quasi-particle-phonon predictions.

We would like to thank Drs. Ch. Stoyanov, A. Vdovin and V.V. Voronov for many stimulating discussions and communication of their results prior to publication and Dr. H. Langevin-Joliot for her help in the DWBA analysis of the high-lying subshells. One of us (CPM) would like to acknowledge the Joliot-Curie Foundation for their financial support during the course of this work.

* Member of the CONICET. On leave from the University of la Plata - ARGENTINE

** Present address : Centre d'Etudes de Bordeaux-Gradignan, Le Haut Vigneau, 33170 GRADIGNAN - FRANCE

REFERENCES

1) O.G. KOVAR, NELSON STEIN and C.K. BOCKELMAN, Nucl. Phys. A231 (1974) 266.

2) R. TICKLE and W.S. GRAY, Nucl. Phys. A247 (1975) 187.

3) S. GALES, C.P. MASSOLO, S. FORTIER, E. GERLIC, J. GUILLOT, E. HOURANI, J.M. MAISON, J.P. SCHAPIRA and B. ZWIEGLINSKI, Phys. Rev. Lett. 48 (1982) 1593.

4) S. GALES, C.P. MASSOLO, S. FORTIER, J.P. SCHAPIRA, P. MARTIN and V. COMPARAT, Phys. Rev. C31 (1985) 94.

5) S. GALES, C.P. MASSOLO, F. AZAIEZ, S. FORTIER, E. GERLIC, J. GUILLOT, E. HOURANI, J.M. MAISON, J.P. SCHAPIRA and G.M. CROWLEY, Phys. Lett. 148 (1984) 323.

6) M. MORLET and A. WILLIS, IPN Orsay Int. Report IPNO-PhN - 7915. J. GUILLOT Thesis. IPN-Orsay 1982.

7) S. GALES, in Proceeding of International School on Nuclear Structure. Alustha, 1985 ed. by V.G. Soloviev and Yu, P. Popov, p. 51.

8) J.R. WU, C.C. CHANG and H.D. HOLMGREN, Phys. Rev. Lett. 40 (1978) 1013.

9) A. BUDZANOWSKI, G. BAUER, C. ALDERLIESTEN, J. BOJOWALD, C. MAYER BÖRICKE, W. DELERT, P. TUREK, F. RÖSEL and D. TRAUTMANN, Phys. Rev. Lett. 41 (1978) 635.

10) R. SERBER, Phys. Rev. 72 (1947) 1008.

11) N. MATSUOKA, A. SHIMIZU, K. HOSONO, T. SAITO, H. SARAGUCHI, A. GOTO, M. KONDO and F. OHTANI, Nucl. Phys. A311 (1978) 173.

12) P.D. KUNZ, University of Colorado, Code DWUCK, unpublished.

13) D.A. GOLOBERG et al., Phys. Rev. C7 (1973) 1938.

14) A. DJALOEIS et al. Nucl. Phys. A306 (1978) 221.

15) N.S. CHANT and J.N. GRAIG, Phys. Rev. C14 (1976) 1763.

16) E. FRIEDMAN, A. MOALEM, D. SURAGUI and S. MORDECHAI, Phys. Rev. C15 (1977) 1604.

17) A. MOALEM, Nucl. Phys. A289 (1977) 45.

18) C.M. VINCENT and H.T. FORTUNE, Phys. Rev. C2 (1970) 782.

19) C.H. STOYANOV, A.I. VDOVIN and V.V. VORONOV ibid. Ref. 6 p. 27. A.I. VDOVIN and CH. STOYANOV, Preprint JINR, 1985, Dubna, E 4-85-352 and private communication.

20) I. HAMAMOTO, Nucl. Phys. A126 (1969) 545, A141 (1970) 11.

21) D. BES and R. BROGLIA, Phys. Rev. C3 (1971) 2389.

22) P. MUKHERJEE, I. MUKHERJEE and R. MAJUMDAR, Nucl. Phys. A294 (1978) 73.

TABLE I

Results from the analysis of the ^{208}Pb (α,^3He) reaction to low-lying states (0-4 MeV)

N°	E_x (MeV)		ℓ	J^π	C^2S		
	Present work	Other works (a)			Present work	Other works (b)	Theoretical predictions
1	0.00	0.00	4	$9/2^+$	0.69	0.94	0.92 (d)
2	0.78	0.779	6	$11/2^+$	0.98	1.05	0.94 (d)
3	1.43	1.424	7	$15/2^-$	0.59	0.57	(0.82 (d) (0.70 (e)
4	2.52	2.493	4	$7/2^+$	0.93	1.05 (c)	0.94 (d)
5	3.05	3.052	7	$15/2^-$	0.054	0.062	0.13 (e)
6	3.59	3.556	7	$15/2^-$	0.037	0.032	0.07 (e)
7	3.73	3.716	7	$15/2^-$	0.035	0.028	0.05 (e)
			(7)	$(15/2)^-$	(0.064)		
8	3.96		(8)	$(17/2)^+$	(0.038)		0.03 (e)
			(7)	$(15/2)^-$	(0.037)		
9	4.22		(8)	$(17/2)^+$	(0.023)		0.03 (e)

(a) Excitation energies have been taken from ref. 1. Only the levels having an energy correspondance with those observed in the present (α,^3He) work are given.

(b) Spectroscopic factors reported in ref. 2

(c) From ref. 1

(d) Theoretical predictions from ref. 19

(e) From ref. 22.

TABLE II

Optical model potential parameters[a]

Channel	V_o (MeV)	r_o (fm)	a_o (fm)	W_o (MeV)	r'_o (fm)	a'_o (fm)	V_{so} (MeV)	r_{so} (fm)	a_{so} (fm)	r_c (fm)
α	155	1.28	0.677	23.2	1.48	0.73	-	-	-	1.4
^3He	115	1.18	0.86	17.2	1.55	0.77	-	-	-	1.4
Bound state parameters[b]										
p	V_n	1.25	0.65	-	-	-	λ:25	1.25	0.65	

(a) Potential of the form :

$$U(r) = -V_o f(x) - iW_o f(x') + V_c \quad \text{where}$$

$$f(x_i) = \left|1 + \exp\left\{\frac{r - r_i A^{1/3}}{a_i}\right\}\right|^{-1}$$

and V_c is the Coulomb potential of a uniform sphere.

(b) Strength (V_n) ajusted to reproduce empircal separation energies
The binding potential is of the form

$$U_n(r) = -V_n \{f(r, r_o A^{1/3}, a_o) - \lambda/45.2 \; 1/r \frac{d}{dr} f(r, r_{so} A^{1/3}, a_{so}) L.S\}$$

where $f(r, r_i A^{1/3}, a_i)$ is the Woods-Saxon form.

TABLE III

Characteristics of the high-lying neutron strengths in ^{209}Pb. Comparison with the prediction from the quasiparticle-phonon nucleon model.

	Theoretical prediction (a)				this work		(d)	
$n\ell j$	ΔE_x	E MeV	σ MeV	C^2S	ΔE_x	C^2S	ΔE_x	C^2S
$2h_{11/2}$	2.0-13.0	6.8	1.88	0.94	4.5-6.5	0.30 (b)	4.5-15	(e)
$1k_{17/2}$	3.0-15.0	8.9	2.26	0.93	9 -15	0.62 (c)	4.5-15	1.15
$1j_{13/2}$	3.0-15.0	9.6	1.72	0.94	6.5-11	1.79 (c)	4.5-15	5.43

(a) See ref. 19.

(b) The analysis is made using a mixture of $\ell = 5$ ($2h_{11/2}$) and $\ell = 7$ ($1j_{15/2}$) in the quoted energy range.

(c) Idem assuming a mixture of $\ell = 7$ ($1j_{13/2}$) and $\ell = 8$ ($1k_{17/2}$) in the corresponding energy regions.

(d) Here, the analysis was made assuming a unique ℓ transfer for the slices located in the indicated energy range.

(e) A pure $\ell = 5$ transfer will not reproduce the experimental angular distributions above 6.5 MeV (see fig. 3).

FIGURE CAPTIONS

Figure 1 : ^{3}He energy spectrum form the ^{208}Pb $(\alpha,^{3}He)$ ^{209}Pb reaction. The numbers at the top of the peaks refer to ^{209}Pb levels. They are listed in table I. The horizontal scale indicates the excitation energy in the ^{209}Pb nuclei. Hatched peaks originate from the $(\alpha,^{3}He)$ reaction on ^{12}C and ^{16}O impurities present in the target. The solid horizontal line indicates the background line shape calculated with the plane-wave break-up model.

Figure 2 : Angular distributions from ^{208}Pb $(\alpha,^{3}He)$ reaction to low lying states in ^{209}Pb. The solid and dashed curves are the LZR-DWBA predictions for the indicated ℓ-values. Each final state is identified by its quantum numbers $n\ell j$ and its excitation energy. The circled numbers refer to the labeling adopted for the nuclear levels in ^{209}Pb (see table I). Vertical bars are statistical errors only.

Figure 3 : Typical angular distribution of slices for three typical excitation energy regions from the ^{208}Pb $(\alpha,^{3}He)$ reaction. The solid and dashed curves are the LZR-DWBA predictions for the indicated ℓ-values. The umbound state form factor has been calculated using the resonance method (see the text). The dot-dashed curves correspond to the substracted background theoretically predicted by the PWBU model. The error bars take into account statistical and systematic errors (see text sect. III).

Figure 4 : (a) Strength functions of the high-lying neutron subshells $2h_{11/2}$, $1j_{13/2}$ and $1k_{17/2}$ in ^{209}Pb (taken from ref. 19).

(b) Comparison between the experimental cross-section for the high-lying states in ^{209}Pb and the predicted theoretical cross-section obtained by the conversion of the theoretical strength functions shown in figure 4.a into double differential cross-sections and summing up all the individual contributions.

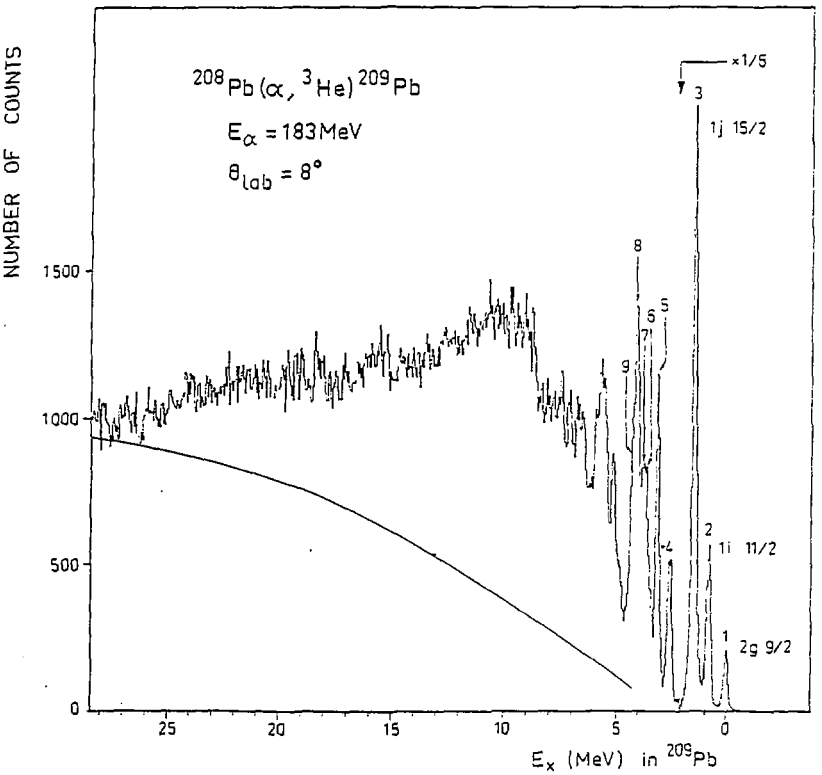
NUMBER OF COUNTS
$^{208}Pb(\alpha, ^3He)^{209}Pb$
$E_\alpha = 183 MeV$
$\theta_{lab} = 8°$
×1/5
3
1j 15/2
8
6
5
7
9
4
2
1i 11/2
1
2g 9/2
1500
1000
500
0
25
20
15
10
5
0
E_x (MeV) in ^{209}Pb

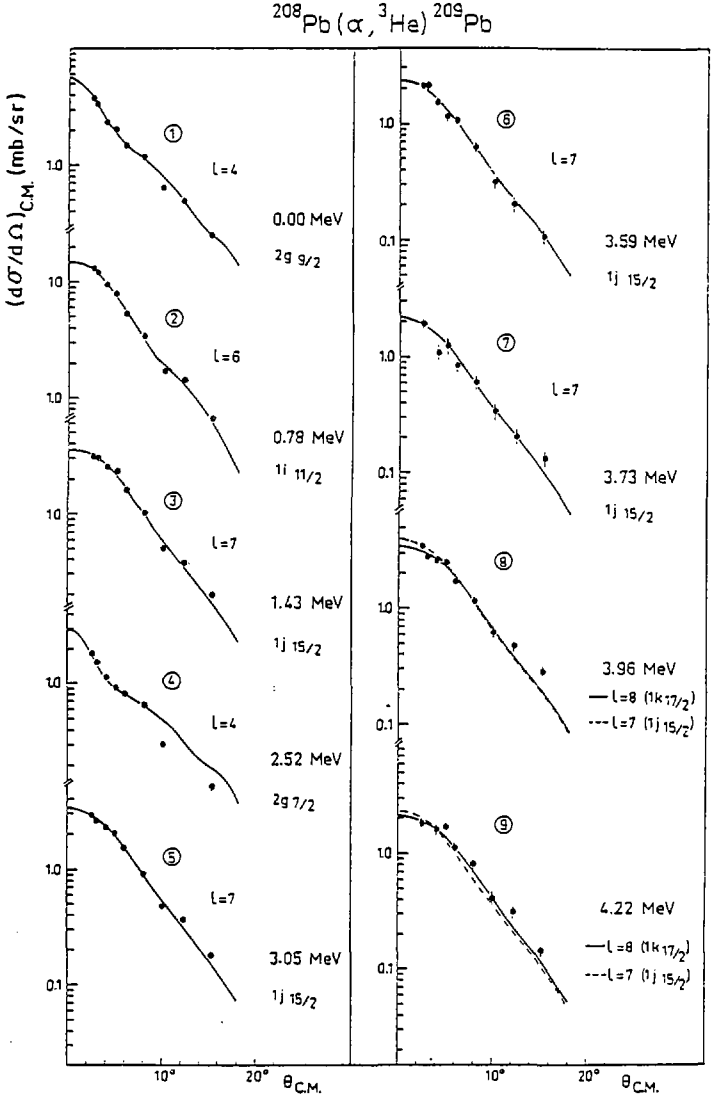
208Pb(α, 3He)209Pb
(dσ/dΩ)C.M. (mb/sr)
θC.M.
①
l=4
0.00 MeV
2g 9/2
②
l=6
0.78 MeV
1i 11/2
③
l=7
1.43 MeV
1j 15/2
④
l=4
2.52 MeV
2g 7/2
⑤
l=7
3.05 MeV
1j 15/2
⑥
l=7
3.59 MeV
1j 15/2
⑦
l=7
3.73 MeV
1j 15/2
⑧
3.96 MeV
—l=8 (1k17/2)
---l=7 (1j 15/2)
⑨
4.22 MeV
—l=8 (1k17/2)
---l=7 (1j 15/2)

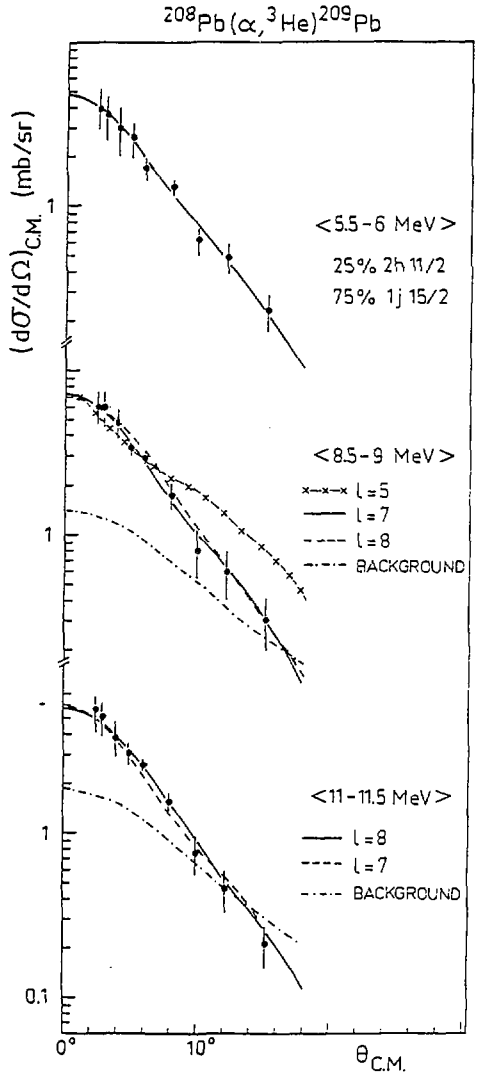
$^{208}Pb(\alpha,{}^{3}He)^{209}Pb$
$(d\sigma/d\Omega)_{C.M.}$ (mb/sr)
1
1
1
0.1
<5.5-6 MeV>
25% 2h 11/2
75% 1j 15/2
<8.5-9 MeV>
l=5
l=7
l=8
BACKGROUND
<11-11.5 MeV>
l=8
l=7
BACKGROUND
0°
10°
$\theta_{C.M.}$

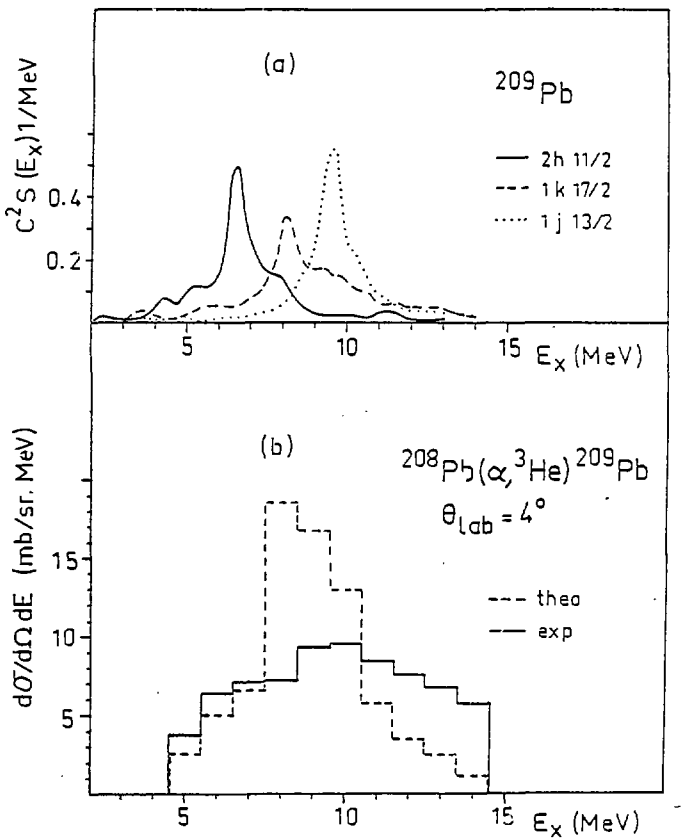
(a)
^{209}Pb
2h 11/2
1k 17/2
1j 13/2
$C^2S\,(E_x)1/MeV$
0.4
0.2
5
10
15
E_x (MeV)
(b)
^{208}Pb(α,^{3}He)^{209}Pb
$\theta_{lab} = 4°$
theo
exp
$d\sigma/d\Omega\,dE$ (mb/sr. MeV)
15
10
5
5
10
15
E_x (MeV)